International Journal of Mass Spectrometry 306 (2011) 241–245

Contents lists available at ScienceDirect

International Journal of Mass Spectrometry

journal homepage: www.elsevier.com/locate/ijms

Absorption of the green fluorescent protein chromophore anion in the gas phase studied by a combination of FTICR mass spectrometry with laser-induced photodissociation spectroscopy

Konstantin Chingin[1], Roman M. Balabin, Vladimir Frankevich, Konstantin Barylyuk, Robert Nieckarz, Pavel Sagulenko, Renato Zenobi*

Department of Chemistry and Applied Biosciences, ETH Zurich, Switzerland

ARTICLE INFO

Article history:
Received 14 August 2010
Received in revised form 14 January 2011
Accepted 18 January 2011
Available online 20 February 2011

Dedicated to Prof. Tino Gäumann on the occasion of his 85th birthday.

Keywords:
GFP chromophore
HBDI anion
Gas-phase absorption
Action spectroscopy
FTICR-MS

ABSTRACT

The optical absorption of the green fluorescent protein chromophore anion ($HBDI^-$) in the gas phase has been addressed by a number of experimental and theoretical studies; however, there is no consensus on its spectral characteristics yet. In this report, the intrinsic absorption of $HBDI^-$ was probed by photo-induced dissociation ("action") spectroscopy using discrete lines of a continuous-wave (CW) laser source. The observed spectral profile of dissociation efficiency revealed a pronounced dependence on the laser irradiance. Dissociation at high irradiance is governed by multiple-photon absorption processes whose efficiency peaks between 476 and 488 nm. At very low irradiance (<0.4 mW cm^{-2}) dissociation of gas-phase $HBDI^-$ is mostly promoted by single-photon transitions and suggests an intrinsic absorption maximum of gas-phase $HBDI^-$ <476 nm, blue-shifted compared to earlier results obtained with pulsed lasers.

1. Introduction

The green fluorescent protein (GFP) is an intrinsically fluorescent protein, which is extensively used as a genetic marker in cellular biology [1]. It has a barrel structure that consists of β-sheets with a chromophore-containing α-helix passing through the center [2,3]. In wild-type GFP, the chromophore 4′-hydroxybenzylidene-2,3-dimethyl-imidazolinone (HBDI) is normally present in either neutral or deprotonated ($HBDI^-$, Scheme 1) form, leading to the absorption bands at around 395 and 480 nm, respectively [4]. The native protein conformation is directly responsible for the bright fluorescence of $HBDI^-$ ($\lambda_{max} \approx 510$ nm, quantum yield ≈0.8, lifetime ≈3 ns) [5], which is weakened by at least three orders of magnitude upon protein unfolding [6]. The underlying mechanisms of the protein–chromophore interaction which enables fluorescence are not entirely understood [7]. It is thought that the protein modulates the chromophore photophysics via both a steric and an electronic influence [8]. The tight packing of the chromophore provided by the native GFP conformation restricts its rotational freedom. The extent of this restriction affects the rate of quenching isomerization reactions in the excited state and has been suggested to directly influence the fluorescence quantum yield [9]. Besides the steric restrictions that the protein interior imposes on the chromophore rotational freedom, a considerable effect on the energy of electronic transitions is expected.

Visible light absorption of $HBDI^-$ in solution is generally significantly blue-shifted compared with the absorption of the $HBDI^-$ chromophore in wt-GFP, consistent with a strong protein–chromophore interaction [10,11]. A multivariant Kamlet–Taft fit [12] of the $HBDI^-$ absorption maxima in different solvents allowed Dong et al. [10] to separate the contributions from selective (H-bonding) as well as from nonselective (dipole–dipole interaction) solvation to the electronic transition. Extrapolation of this fit to both zero hydrogen bond donor/acceptor properties and zero polar solvation parameters yields an estimate for the intrinsic absorption maximum of $HBDI^-$ in the absence of solvent around 437 nm, which is ca. 45 nm blue-shifted relative to the absorption of $HBDI^-$ inside the protein. A very similar estimate was obtained (440 ± 5 nm) upon direct extrapolation of absorption maxima measured in non-polar solvents to the dielectric constant of vacuum, $\varepsilon = 1$ [13]. Unfortunately, there is no single solvent parameter which adequately describes the solvatochromism of $HBDI^-$ [7]. There-

* Corresponding author. Tel.: +41 44 632 4376; fax: +41 44 632 1292.
E-mail address: zenobi@org.chem.ethz.ch (R. Zenobi).
[1] Current address: Department of Chemistry, Stanford University, Stanford, CA 94305, United States.

1387-3806/$ – see front matter © 2011 Elsevier B.V. All rights reserved.
doi:10.1016/j.ijms.2011.01.014

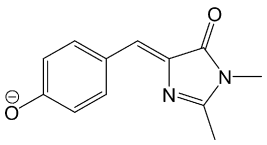

Scheme 1. Anionic form of the model GFP chromophore, HBDI.

fore, the bathochromic shift in the absorption of $HBDI^-$ inside the protein cannot be entirely assigned to a specific interaction (e.g., H-bonding) but rather reflects a unique microenvironment provided by the protein interior.

The effect of the protein on the electronic transition energies in $HBDI^-$ deduced from solution-phase experiments has been questioned by the results of pioneering action spectroscopy experiments carried out on $HBDI^-$ in the gas phase by the groups of Andersen [14,15] and Jockusch [16]. In these experiments, gas-phase $HBDI^-$ ions trapped inside an electrostatic storage ring [14] or a quadrupolar ion trap [16] were exposed to irradiation produced by a tunable laser source. Both ionic [16] and neutral [14] fragment yields as well as parent ion depletion [16] were monitored as a function of the excitation wavelength and revealed a maximum at around 480 nm, which is very close to the absorption maximum of $HBDI^-$ in the protein. It was therefore proposed by Andersen and coworkers that the GFP scaffold offers a near-vacuum environment for the chromophore, although with restrictions on its rotational freedom [14]. In our opinion, this conclusion is quite speculative, as the lack of a shift in an electronic transition does not automatically imply that "the actual environment of the chromophore inside the protein cavity is much closer to vacuum than to bulk solution" [14]. In fact, the absorption of $HBDI^-$ in DMSO and DMF was also found to be very similar to that in the protein [10,17]. The observation alone, that $HBDI^-$ optical absorption maximum in the gas phase deduced from action spectroscopy (≈480 nm) is very different from that extrapolated from solution-phase studies (≈440 nm), is quite unsettling. A key difference between the solution-phase measurements and those in the gas phase is that multiple-photon processes may become important in the latter [16]. For a more accurate determination of the absorption at $\varepsilon = 1$ (vacuum), the contribution of these multiple-photon processes needs to be minimized, by employing lower optical power. In order to achieve single-photon activation in action spectroscopy experiments with pulsed laser sources, the irradiation energy within each single pulse would have to be attenuated down to the energy level delivered by CW sources. However, given the low duty cycle of pulsed sources, on the order of 10^{-6}, the time needed to produce detectable fragmentation would become exceedingly long, especially when compared with the typical storage time that is possible with an ion trap mass spectrometer.

To contribute to the clarification of these questions, we present here the results of photoabsorption action spectroscopy experiments performed on $HBDI^-$ ions trapped inside the Penning trap of a Fourier-transform ion cyclotron resonance mass spectrometer (FTICR-MS) using low power, continuous-wave (CW) laser irradiation.

2. Experimental

The experimental setup for laser spectroscopy of gas-phase ions has recently been described in detail [18]. $HBDI^-$ ions (m/z 215) were produced by electrospray ionization and then trapped inside the ICR cell (base pressure = 5×10^{-9} mbar). Trapped ions were excited with discrete lines of an Ar^+ ion laser (458, 476, 488, 496 and 502 nm). The laser excitation was started 10 s after the ion introduction into the ICR cell to allow time to restore the base pressure. The laser beam size was expanded to ca. 1.5 cm in diameter using a lens system in order to ensure full overlap with the ion cloud

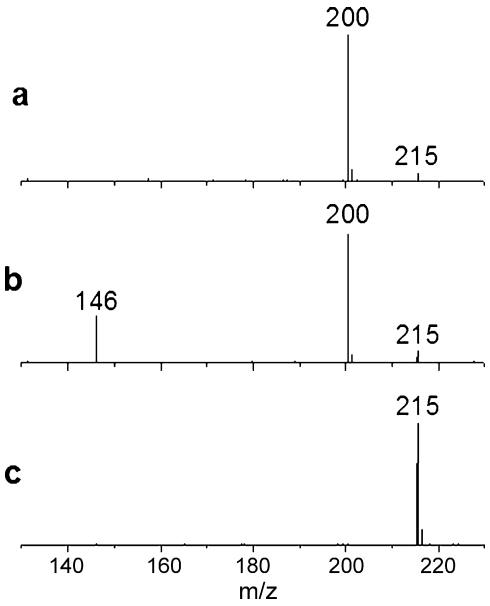

Fig. 1. Photodissociation pathways of gas-phase $HBDI^-$: (a) the major ionic fragment formed by neutral methyl loss from of $HBDI^-$ is directly detected by FTICR-MS at m/z 200; (b) photodetached electrons are revealed via the capture reaction with neutral SF_6 gas to form SF_6^- anion, which is detected by FTICR-MS (m/z 146); (c) in the presence of SF_6 gas only the parent $HBDI^-$ species are observed (m/z 215) when the laser is blocked, indicating that the SF_6^- anions in (b) are specifically formed from the reaction with electrons detached from HBDI.

(diam. ~3 mm). Depletion of the parent $HBDI^-$ ion signal in the mass spectrum, $I(m/z\,215)/I_0(m/z\,215)$, was monitored as a function of the excitation wavelength [16]. The notation $I(m/z\,x)$ is used here and below refers to the ion intensity of the ions of species x in the mass spectrum. An index '0' is used to denote reference ion intensities obtained at zero laser irradiance over the same trapping time. Every measurement was repeated five times. The limited number of available wavelengths in our experiments does not allow us to record dissociation spectra with high spectral resolution; however, the position of the maximum can still be assessed.

In the electron capture experiments (Section 3.1), SF_6 gas was introduced into the ICR cell via a regulated mechanical leak valve, and its pressure was maintained at 4×10^{-8} mbar over the entire interval of laser exposure (2 min).

3. Results and discussion

3.1. Photodissociation pathways

Two major fragmentation channels exist for gas-phase $HBDI^-$ when exposed to laser irradiation, neutral methyl loss (fragment ion at m/z 200, Fig. 1a) and photoelectron detachment (*ePD*), in agreement with the findings of Forbes and Jockusch [16]. To detect the detached electrons we used SF_6 buffer gas, which efficiently traps low-energy electrons to form SF_6^- [19] (peak at m/z 146, Fig. 1b). No SF_6^- ions were detected in a reference experiment in which SF_6 gas was introduced, but the laser was blocked (Fig. 1c). It is worth noting that the operation of the *ePD* mechanism could not be rigorously proven in earlier experiments, since neither the detached electron nor the neutral product can be directly detected in ion trap mass spectrometers [16]. Use of electron capture by SF_6 is an elegant way to circumvent this problem.

3.2. Power dependence of photodissociation

In order to investigate the effect of the laser irradiance on the measured maximum of photodissociation for $HBDI^-$, a series of

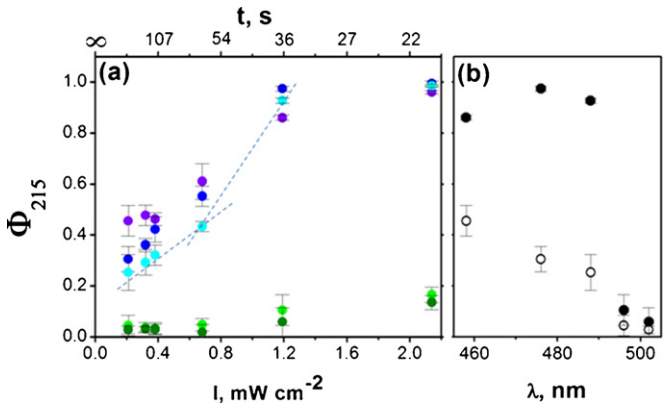

Fig. 2. (a) Dependence of the fragmentation yield, $\Phi_{215} = 1 - I(m/z\,215)/I_0(m/z\,215)$, on CW laser irradiance (I) for gas-phase $HBDI^-$ anions at different excitation wavelengths (violet, 458 nm; dark blue, 476 nm; cyan, 488 nm; light green, 496 nm; dark green, 502 nm). All the data points we obtained at a constant laser fluence ($F = 43\ mJ\ cm^{-2}$), while the irradiance was varied. In order to keep the laser fluence constant, the increase in irradiance was in each case compensated by a corresponding decrease in the exposure time (t) (e.g., $0.215\ mW\ cm^{-2} \cdot 200\ s = 43\ mJ\ cm^{-2}$). (b) Wavelength dependence of photodissociation for gas-phase $HBDI^-$ obtained upon exposure of trapped ions to CW laser irradiance of 0.215 (open circles) and 1.194 $mW\ cm^{-2}$ (closed circles) power over 200 and 36 s correspondingly.

measurements were performed in which laser irradiance (I) and exposure time (t) were simultaneously varied such that a constant laser fluence (F) was maintained, $F = It = 43\ mJ\ cm^{-2}$. Under these experimental conditions, the final parent ion depletion is expected to be independent of irradiance for a single photon process, while it should grow with laser irradiance for a multiple-photon absorption process. Fig. 2a shows the dependence of the fragmentation yield, $\Phi_{215} = 1 - I(m/z\ 215)/I_0(m/z\ 215)$, for $HBDI^-$ on laser irradiance for five different excitation wavelengths. The fragmentation yields of $HBDI^-$ are also plotted as a function of excitation wavelength at two different values of irradiance, to obtain a spectral trend representation (Fig. 2b).

The fragmentation yield in Fig. 2a clearly grows as a function of laser irradiance at each wavelength until it saturates near $\Phi_{215} = 1$ (all the parent $HBDI^-$ ions are destroyed), indicating that ion fragmentation occurs mainly via multiple-photon absorption (see above). Note that data points obtained in the saturation regime ($I > 2\ mW\ cm^{-2}$ for 458, 476, and 488 nm in Fig. 2a) are indeed no longer indicative of a dissociation rate law. As the laser irradiance is decreased, single-photon fragmentation becomes more pronounced. This can be deduced from the decreasing slope of the fragment yield *vs.* laser irradiance (Fig. 2a, dashed line). A non-zero fragment yield of $HBDI^-$ is predicted even for vanishingly low laser irradiance (but infinitely long exposure time) at 458, 476 and 488 nm (Fig. 2a), suggesting that the single-photon dissociation channel is accessible at these excitation wavelengths. In contrast, extrapolation of the fragment yield dependence at 496 and 502 nm to zero irradiance yields a near-zero fragmentation rate, indicating that the energy of a single photon is below the threshold energy of both dissociation channels (*ePD* and methyl loss), in a good agreement with the theoretical estimate (B3LYP/6-311+G**) of 2.5 eV [16].

The spectral trend obtained upon excitation with 1.2 $mW\ cm^{-2}$ (strong multiple-photon character) implies a dissociation maximum between 476 and 488 nm (Fig. 2b, solid circles), which is in very good agreement with the results of earlier photoabsorption action spectroscopy experiments [14,16]. Both the sharp edge of the spectrum at ~496 nm and the tailing to the blue agrees well with the observations by Forbes and Jockusch [16]. In their experiments, trapped $HBDI^-$ ions were excited by a train of low-energy sub-picosecond pulses ($\tau = 130$ fs; $E = 50$ pJ/pulse; $P_{total} = 4$ mW; $\tau_{total} = 250$ ms). These authors also concluded that dissociation of $HBDI^-$ mostly proceeded via multiple-photon absorption around 480 nm, while single-photon dissociation was thought to be operating in the deep-blue region of the spectrum [16]. The close agreement of the spectral representation obtained upon activation with CW laser irradiance of 1.2 $mW\ cm^{-2}$ with the results of pulsed-excitation experiments reflects that multiple-photon absorption governs the photofragmentation process under these conditions. In other work, Andersen and coworkers induced dissociation of gas-phase $HBDI^-$ ions trapped in a storage ring by a single laser pulse of high energy ($\tau = 3$ ns, $E = 1$–2 mJ). In this work, it was reported that $HBDI^-$ photodissociates as a result of single-photon absorption at 495 nm [15], which is quite surprising given the high peak power of the excitation (~0.5 MW). The reason that their observations were interpreted as single-photon dissociation could be due to the fact that the products of *ePD* were not observed to any appreciable extent in the storage ring [16]. This was also proposed [16] to account for the absence of the blue tailing in the spectrum recorded by Andersen and coworkers [14,15]. Besides that, it was noted by the authors that it was exceedingly difficult to establish the correct power dependence of the neutral yield in pulsed experiments [15]. In earlier work from the same group on the absorption of gas-phase $HBDI^-$, two-photon dissociation was reported [14].

While the spectral profile recorded at 1.2 $mW\ cm^{-2}$ excitation laser irradiance shows a maximum at ca. 480 nm, the dependence recorded at 0.2 $mW\ cm^{-2}$ reveals a gradual decrease from 458 to 488 nm (Fig. 2b, open circles). We interpret this remarkable difference between the two profiles to be due to the large contribution from single-photon dissociation upon excitation with 0.2 $mW\ cm^{-2}$. Below we evaluate to what extent photodissociation profiles obtained in the low- and high-power regimes are relevant to the optical absorption of $HBDI^-$ in the gas phase.

3.3. Multiple-photon dissociation

Multiple-photon dissociation of $HBDI^-$ can proceed via a number of pathways. Below two possible two-photon schemes are considered as examples. It is worth noting, however, that the absorption of more than two photons can be involved in dissociation, especially at higher laser fluences. Absorption of the first photon promotes $HBDI^-$ to the first excited electronic state. Theoretical calculations suggest that in the excited state $HBDI^-$ ions assume a new, twisted, conformation [20]. Absorption of the second photon, which induces dissociation, may therefore take place from this new state. Alternatively, the excited electronic state of $HBDI^-$ can be deactivated via internal conversion to a high vibrational level of the ground electronic state. In the absence of efficient collisional cooling in ultra-high vacuum, absorption of the second photon can then occur from this vibrationally hot state. The latter mechanism is supported by the observed pressure dependence of multiple-photon dissociation kinetics for gas-phase $HBDI^-$ [21]. In both cases considered, the observed dissociation spectrum contains contributions from the ground-state absorption of $HBDI^-$ (first photon) as well as from the optical absorption of the state from which the dissociative transition occurs (second photon); only the first contribution is characteristic of the linear absorption of $HBDI^-$. The photoabsorption action spectrum of gas-phase $HBDI^-$ obtained by Forbes and Jockusch using pulsed excitation consists of two bands with maxima at ~480 nm and ~450 nm [16]. The authors assigned the 480 nm band to the $S_0 \rightarrow S_1$ adiabatic transition and the one at 450 nm to a highly active vibrational mode of the excited state ($+1450\ cm^{-1}$) [16]. The peak at 480 nm was identified to result from multiple-photon absorption, while a significant contribution from single-photon dissociation to the second band was expected [16].

Based on the results presented here, the resonance around 480 nm present in the earlier action spectroscopy experiments

could alternatively be interpreted to be due to transition from the twisted intermediate state or hot vibrational level of the ground state, as proposed above. If this is true, then the maxima in the spectra obtained in the multiple-photon absorption regime can be explained by a superposition of bands corresponding to the $S_0 \rightarrow S_1$ as well as to the aforementioned transitions and is in this case not representative of vibronic structure of the linear absorption spectrum. In the condensed phase, the vibronic structure of the electronic spectra for HBDI$^-$ can become quite distinct if the *cis–trans* izomerization channels in the excited state are suppressed, e.g., inside the protein at low temperatures [22] or in some glasses [17]. The suppression of isomerization in the excited state of HBDI$^-$ imposed by the restriction of rotational freedom is also thought to be a key contributor to the high fluorescence yield [22]. The fact that no fluorescence has been observed for gas-phase HBDI$^-$ ions [16] suggests that the isomerization channel does operate in the excited state, which should result in a solution-like, unresolved spectrum at room temperature.

Another inevitable drawback of using multiple-photon dissociation as a probe of optical absorption for HBDI$^-$ is that different dissociation channels having both different power dependence and spectral profiles operate simultaneously, i.e., single- and *n*-photon dissociation (Fig. 2b). The shape of the resulting dissociation spectrum becomes dependent on the excitation power in this case. At high power, the contribution of multiple-photon dissociation ($n > 1$) associated with the band at 480 nm in the spectrum dominates [16]. At very low powers, the contribution from multiple-photon processes vanishes, and the maximum is shifted to lower wavelengths (Fig. 2b, open circles). Any intermediate spectral shape can result from varying the excitation laser power.

3.4. Single-photon dissociation

The dissociation spectral profile obtained in the low-power regime suggests an absorption maximum of gas-phase HBDI$^-$ anions at shorter wavelengths than 476 nm (Fig. 2b, open circles). Because of the discrete number of excitation wavelengths in our experiments, we cannot conclude whether the maximum occurs between 458 and 476 nm or at even shorter wavelengths (<458 nm). Note that irradiation at $\lambda \geq 496$ nm cannot induce fragmentation of gas-phase HBDI$^-$ ions in the single-photon regime, since the photon energy is below the dissociation threshold. The optical absorption of HBDI$^-$ thus cannot be derived from action spectroscopy above $\lambda \approx 496$ nm, which explains the apparent discontinuity in this data (Fig. 2b, open circles). The position of the maximum (<476 nm) is at least 20 nm away from the red edge of the spectrum (>500 nm). This considerable shift suggests that the absorption maximum of HBDI$^-$ in the gas phase does not correspond to the shortest adiabatic transition. The same phenomenon was found for HBDI$^-$ both in solution and inside wt-GFP, based on the results of fluorescence spectroscopy experiments carried out at different temperatures [17,22]. The fact that the shortest adiabatic transition is not the most intense in the spectrum is very important, as it suggests a significant structural change between the ground and excited states [17], which is central in theoretical models of ultrafast radiationless decay in HBDI [23]. The position of the absorption maximum for free HBDI$^-$ predicted in the low-power regime is consistent with a maximum at ≈437 nm extrapolated from solution-phase data based on Kamlet–Taft fit [10]. For the single-photon dissociation of HBDI$^-$ to be a reliable characteristic of optical absorption, it is important that every photon absorbed induces dissociation with equal efficiency. This may not be the case for HBDI$^-$: dissociation (*ePD* or methyl loss) at 458 nm can occur faster than at 488 nm, and therefore a part of the ions excited at 488 nm will have sufficient time to undergo internal conversion back to the ground state. In other words, the fragmentation

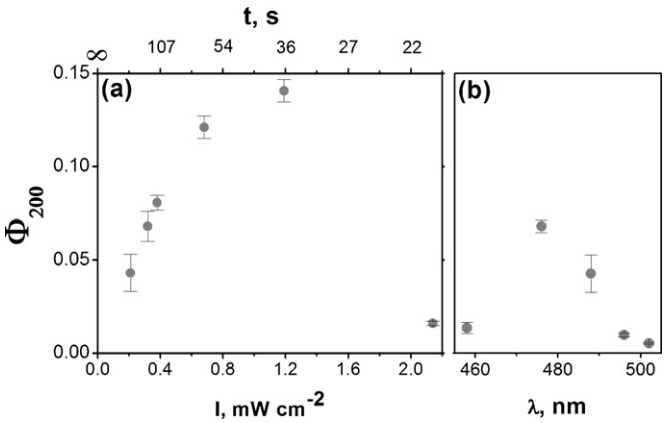

Fig. 3. (a) Yield of the HBDI$^-$ fragment formed by the neutral methyl loss, $\Phi_{200} = I(m/z\ 200)/I_0(m/z\ 215)$, as a function of laser irradiance at 488 nm. (b) Yield of m/z 200 ions as a function of excitation wavelength in the low-power dissociation mode (0.2 mW cm^{-2}).

yield of HBDI$^-$ at 488 nm would underestimate the absorption cross-section. Detailed knowledge of the time scales of *ePD*, neutral methyl loss, and internal conversion pathways may be needed to determine whether single-photon dissociation reliably reflects the intrinsic optical absorption of HBDI$^-$.

Unfortunately, HBDI$^-$ represents a very difficult case for ab initio methods. The results are extremely method-dependent. For example, CASPT2 calculations with the same basis set (6-31G*) and size of the CAS yielded an estimate for the vertical $S_0 \rightarrow S_1$ transition energy of HBI$^-$ (HBDI$^-$ sans 2×CH$_3$) of 2.63 (471 nm) or ∼ 2.9 eV (428 nm) [13], depending on the zero-order Hamiltonian employed. It is also noteworthy that the precision of CASSCF calculations used to simulate the absorption spectrum of HBI$^-$ [20] is greatly limited for a number of reasons, e.g., because correlation effects in the HF wave functions are neglected. Accounting for the correlation effects, however, would be important for reliably predicting the excitation energy [24,25]. Most recent state-of-the-art theoretical calculations utilizing different computational algorithms (TDDFT, CASPT2, QMC) consistently predict a vertical excitation energy of HBDI$^-$ around 2.9–3.0 eV (415–428 nm) [13]. This estimate agrees reasonably well with the extrapolation from solution-phase measurements (437 nm) [10] and the results of our action spectroscopy in the low-power regime (<476 nm). To what extent available theoretical predictions take into account the dissociative nature of the excited state is not yet clear [26].

3.5. Spectral representation of dissociation channels

Fig. 3a demonstrates the yield of the fragment formed by the neutral methyl loss, $\Phi_{200} = I(m/z\ 200)/I_0(m/z\ 215)$, as a function of laser irradiance at 488 nm. It can be seen that the signal in the mass spectrum corresponding to the fragment m/z 200 grows at low laser irradiance while it starts to decay at higher irradiance. This observation is explained by the fact that the fragment at m/z 200 also absorbs visible light and can also undergo *ePD*. When exposed to laser irradiation, the number of parent HBDI$^-$ ions in the cell continuously decreases (Fig. 2a, cyan color), which results in slower formation of the fragment, $dI(m/z\ 200)/dt \sim I(m/z\ 215)$. At some point, the fragmentation rate of m/z 215 ions becomes lower than the rate of *ePD* from m/z 200 ions, and the number of m/z 200 ions starts to decrease. The dissociative nature of the fragment m/z 200 renders it difficult to precisely account for the contribution of the *ePD* and neutral methyl loss dissociation channels in HBDI$^-$ in the multiple-photon absorption regime. Thus, it is quite possible that

the intensity of the band at 480 nm in the *ePD* spectrum reported by Forbes and Jockusch [16] is exaggerated due to *ePD* from m/z 200 ions. It is worth noting that even at low powers, when the parent $HBDI^-$ ions undergo single-photon dissociation, daughter ions can still fragment on the time scale of the experiment due to faster dissociation kinetics. Fig. 3b shows the yield of m/z 200 ions as a function of excitation wavelength in the low-power dissociation mode (0.2 mW cm^{-2}). The yield peaks around 480 nm, which is in agreement with the observation by Forbes and Jockusch [16]. The contribution of *ePD* to the fragmentation yield of $HBDI^-$ anions can be calculated as $\Phi_{ePD} = \Phi_{215} - \Phi_{200}$. In the low-power regime, the photodissociation spectrum of $HBDI^-$ (Fig. 2b, open circles) is largely dictated by *ePD*, which is a faster process than the methyl loss. The relative contribution of *ePD* is particularly large at low excitation wavelengths (e.g., 458 nm). The contribution of methyl loss becomes more notable at higher wavelengths (e.g., 488 nm), probably because of decreasing efficiency for the competing *ePD* channel close to its energy threshold [16]. At higher excitation wavelengths (e.g., 496 and 502 nm), neither dissociation channel can be accessed in the single-photon regime, and both Φ_{ePD} and Φ_{200} rapidly approach zero – hence is the observed peak for Φ_{200} in Fig. 3b.

4. Conclusions

The spectral trend of photodissociation of gas-phase $HBDI^-$ ions reveals a clear dependence on excitation laser power. In our opinion, neither the single- nor the multiple-photon dissociation regime can reliably represent the optical absorption spectrum of $HBDI^-$. While the absorption predicted by photodissociation experiments in the low-power regime is consistent with solution-phase observations, a better understanding of dissociation mechanisms is still necessary to validate the correlation between dissociation and optical spectra.

Acknowledgements

We thank Kyril Solntsev for providing HBDI and Claudia Filippi, Anna Krylov and Stephen Meech for helpful discussions. Financial support from ETH Zurich (TH Grant No. TH-20 06-1 to RZ) is gratefully acknowledged. Prof. Tino Gäumann is acknowledged for facilitating the transfer of a 4.7 T superconducting magnet to RZ's group in 1994; this work was carried out on an FTICR mass spectrometer, which still uses this magnet.

References

[1] R.Y. Tsien, The green fluorescent protein, Annu. Rev. Biochem. 67 (1998) 509–544.
[2] M. Ormo, A.B. Cubitt, K. Kallio, L.A. Gross, R.Y. Tsien, S.J. Remington, Crystal structure of the Aequorea victoria green fluorescent protein, Science 273 (1996) 1392–1395.
[3] F. Yang, L.G. Moss, G.N. Phillips, The molecular structure of green fluorescent protein, Nat. Biotechnol. 14 (1996) 1246–1251.
[4] T.M.H. Creemers, A.J. Lock, V. Subramaniam, T.M. Jovin, S. Volker, Three photoconvertible forms of green fluorescent protein identified by spectral hole-burning, Nat. Struct. Biol. 6 (1999) 557–560.
[5] G. Striker, V. Subramaniam, C.A.M. Seidel, A. Volkmer, Photochromicity and fluorescence lifetimes of green fluorescent protein, J. Phys. Chem. B 103 (1999) 8612–8617.
[6] H. Niwa, S. Inouye, T. Hirano, T. Matsuno, S. Kojima, M. Kubota, M. Ohashi, F.I. Tsuji, Chemical nature of the light emitter of the Aequorea green fluorescent protein, Proc. Natl. Acad. Sci. U.S.A. 93 (1996) 13617–13622.
[7] S.R. Meech, Excited state reactions in fluorescent proteins, Chem. Soc. Rev. 38 (2009) 2922–2934.
[8] S.L. Maddalo, M. Zimmer, The role of the protein matrix in green fluorescent protein fluorescence, Photochem. Photobiol. 82 (2006) 367–372.
[9] C.M. Megley, L.A. Dickson, S.L. Maddalo, G.J. Chandler, M. Zimmer, Photophysics and dihedral freedom of the chromophore in yellow, blue, and green fluorescent protein, J. Phys. Chem. B 113 (2009) 302–308.
[10] J. Dong, K.M. Solntsev, L.M. Tolbert, Solvatochromism of the green fluorescence protein chromophore and its derivatives, J. Am. Chem. Soc. 128 (2006) 12038–12039.
[11] K.L. Litvinenko, N.M.S.R. Webber, Meech, Ultrafast excited state relaxation of the chromophore of the green fluorescent protein, B. Chem. Soc. Jpn. 75 (2002) 1065–1070.
[12] M.J. Kamlet, J.L.M. Abboud, M.H. Abraham, R.W. Taft, Linear solvation energy relationships. 23. A comprehensive collection of the solvatochromic parameters, pi-star, alpha and beta, and some methods for simplifying the generalized solvatochromic equation, J. Org. Chem. 48 (1983) 2877–2887.
[13] C. Filippi, M. Zicchedu, F. Buda, Absorption Spectrum of the green fluorescent protein chromophore: a difficult case for ab initio methods? J. Chem. Theory Comput. 5 (2009) 2074–2087.
[14] S.B. Nielsen, A. Lapierre, J.U. Andersen, U.V. Pedersen, S. Tomita, L.H. Andersen, Absorption spectrum of the green fluorescent protein chromophore anion in vacuo, Phys. Rev. Lett. 87 (2001).
[15] L.H. Andersen, H. Bluhme, S. Boye, T.J.D. Jorgensen, H. Krogh, I.B. Nielsen, S.B. Nielsen, A. Svendsen, Experimental studies of the photophysics of gas-phase fluorescent protein chromophores, Phys. Chem. Chem. Phys. 6 (2004) 2617–2627.
[16] M.W. Forbes, R.A. Jockusch, Deactivation pathways of an isolated green fluorescent protein model chromophore studied by electronic action spectroscopy, J. Am. Chem. Soc. 131 (2009) 17038–17039.
[17] N.M. Webber, S.R. Meech, Electronic spectroscopy and solvatochromism in the chromophore of GFP and the Y66F mutant, Photoch. Photobio. Sci. 6 (2007) 976–981.
[18] K. Chingin, H.W. Chen, G. Gamez, R. Zenobi, Exploring fluorescence and fragmentation of ions produced by electrospray ionization in ultrahigh vacuum, J. Am. Soc. Mass Spectrom. 20 (2009) 1731–1738.
[19] R.K. Asundi, J.D. Craggs, Electron capture + ionization phenomena in $SF_6 + C_7F_{14}$, Proc. Phys. Soc. Lond. 83 (1964) 611.
[20] M.E. Martin, F. Negri, M. Olivucci, Origin, nature, and fate of the fluorescent state of the green fluorescent protein chromophore at the CASPT2//CASSCF resolution, J. Am. Chem. Soc. 126 (2004) 5452–5464.
[21] M. Forbes, C. Yeung, C. Yang, V. Dong, R. Jockusch, 57th ASMS Conference on Mass Spectrometry and Allied Topics, Philadelphia, PA, 2009.
[22] S.S. Stavrov, K.M. Solntsev, L.M. Tolbert, D. Huppert, Probing the decay coordinate of the green fluorescent protein: arrest of *cis–trans* isomerization by the protein significantly narrows the fluorescence spectra, J. Am. Chem. Soc. 128 (2006) 1540–1546.
[23] D. Mandal, T. Tahara, S.R. Meech, Excited-state dynamics in the green fluorescent protein chromophore, J. Phys. Chem. B 108 (2004) 1102–1108.
[24] O. Rubio-Pons, O. Loboda, B. Minaev, B. Schimmelpfennig, O. Vahtras, H. Agren, CASSCF calculations of triplet state properties: applications to benzene derivatives, Mol. Phys. 101 (2003) 2103–2114.
[25] S. Fantacci, A. Migani, M. Olivucci, CASPT2//CASSCF and TDDFT//CASSCF mapping of the excited state isomerization path of a minimal model of the retinal chromophore, J. Phys. Chem. A 108 (2004) 1208–1213.
[26] E. Epifanovsky, I. Polyakov, B. Grigorenko, A. Nemukhin, A.I. Krylov, Quantum chemical benchmark studies of the electronic properties of the green fluorescent protein chromophore. 1. Electronically excited and ionized states of the anionic chromophore in the gas phase, J. Chem. Theory Comput. 5 (2009) 1895–1906.